Report for

Temperature and Humidity Monitoring Board for $\overline{\text{P}}$ANDA (THM$\overline{\text{P}}$)

(AntiProton Annihilations at Darmstadt)

Strong Interaction Studies with Antiprotons

F. Feldbauer, P. Friedel
Ruhr-Universität **Bochum**, Institut für Experimentalphysik I, Germany

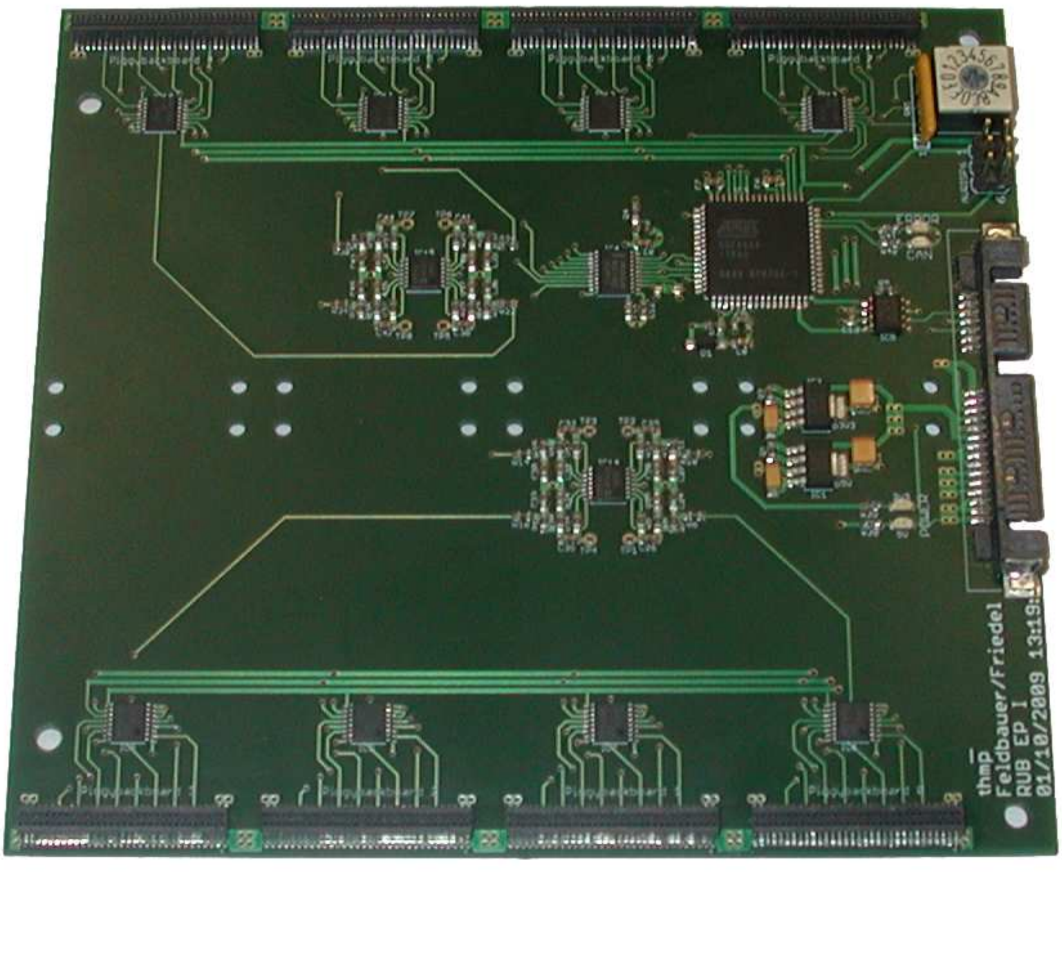

Cover: The picture shows the $\mathsf{THM\overline{P}}$ mainboard. The dimensions of the mainboard are (120×130) mm^2. The eight connectors for the piggyback boards are placed on the left and right side of the PCB. Next to them the 8:1 multiplexers are located. At the front the power and CAN-Bus connectors and the main ICs, the microcontroller and the ADC are mounted.

Abstract

This document presents the development and tests of the Temperature and Humidity Monitoring Board for $\overline{\mathsf{P}}$ANDA (THM$\overline{\mathsf{P}}$).
The THM$\overline{\mathsf{P}}$ has been developed to monitor the temperature and humidity inside the electromagnetic calorimeter (EMC) of the $\overline{\mathsf{P}}$ANDA target spectrometer. Therefore it has 64 channels and is designed to read out PT100 temperature sensors and HIH-4000 humidity sensors. This device has been constructed to operate in a temperature range from $-30\,^{\circ}\mathrm{C}$ to $+30\,^{\circ}\mathrm{C}$. To cover the whole temperature range of the EMC, the measurement range will also be from $-30\,^{\circ}\mathrm{C}$ to $+30\,^{\circ}\mathrm{C}$ with a resolution of 0.05 K. The relative humidity (RH) can be measured in the range from 0 to 100% RH with an accuracy of 3.5%. For the read-out of this device a CAN interface is foreseen.
The THM$\overline{\mathsf{P}}$ should fulfill the environmental requirements of operating in the cooled area of the EMC. Different tests were carried out to verify this.

Contents

1 Motivation

At $-25\,^{\circ}\mathrm{C}$, the light yield of PWO depends heavily on the temperature with a change of 3%/K. Therefore, the temperature of the crystals has to be stabilized and monitored to ensure the temporal and spacial homogeneity of the calorimeter as well as to diagnose and control the longitudinal temperature distribution along one crystal. When setting an upper limit for the impairment of the energy resolution $\sigma_{E,\,\mathrm{temporal}} \leq 0.2\%$ caused by *temporal* variation of the crystal temperatures, one obtains a requirement for the temporal homogeneity of the calorimeter:

$$\sigma_T = \frac{0.2\%}{3\,\%/\mathrm{K}} \approx 0.07\,\mathrm{K} \qquad , \tag{1.1}$$

which leads to a demand of a temporal homogeneity of about 0.05 K.
Adding to the temporally induced decrease in energy resolution, one also has to take into account the spacial inhomogeneities. Simulations show a maximum allowance for the temperature gradient along a crystal of 0.01 K/mm [Zh09].
Another quite important point is the humidity inside the calorimeter. If ice forms on the crystal's surface total reflection is no longer provided and therefore the light yield decreases. This is why one has to flush the whole calorimeter with dry nitrogen and monitor the relative humidity inside.
For monitoring the temperature and humidity, the THM$\overline{\mathrm{P}}$ (**T**emperature and **H**umidity **M**onitoring Board for **P**ANDA) was developed.

2 Temperature and Humidity Sensors

2.1 Development of ultra-thin Platinum Temperature Sensors

The space in one of the four 2×2-subcompartments of a 4×4-subunit is very limited, and it is even more reduced due to a further stabilizing carbon fiber cross and the DF2000MA mirror foil, which envelopes each crystal. Furthermore, the option is discussed to wrap each 2×2 crystal package in a metallized and grounded foil for improved shielding of RF noise.
To be still able to check the temperature in the vicinity of the crystals, a very thin sensor has to be developed. The space available is $80\,\mu$m at maximum, and the temperature resolution has to be in the order of 0.05 K. Prototypes for such sensors have been developed, ref. [Sc09] and are being presented on the following pages of this report.

2.1.1 Design of the Temperature Sensors

The idea is to measure the resistance change in a thin platinum wire to express the temperature change. Platinum is used for two reasons: first, it has a rather high specific resistance ($\rho = 110 \cdot 10^{-9}\,\Omega$m), a fact which reduces the needed wire length in contrast to a material with lower specific resistance. Second, the large temperature coefficient of the resistance change of $3.88 \times 10^{-3}\,\mathrm{K}^{-1}$ leads to well measurable resistance changes, while the temperature only shifts marginally.
The measurement is to take place via a four-terminal sensing, which is presented in the next section. This method allows that the resistance of the supply wires to the point where the sensor starts be ignored. This is a common method to ensure high-precision resistance measurements.
The platinum wire is brought onto a self-adhesive Kapton film and covered with a non-adhesive film on the reverse side. Up to now, such highly specialized sensors are not available on the market, so they have to be developed by the $\overline{\mathrm{P}}$ANDA Collaboration.
The choice of wire diameters is quite relevant. On the one hand, a thin wire has the advantage of saving wire length while having the same resistance. In addition, the height of the sensor is reduced by using a thin wire. On the other hand, a thin platinum wire tends to tear at only small tensions, so that the wire has to be applied with special precaution. It has been investigated that a 25 μm wire is a fair compromise.
The resistance of the sensor at $0\,^{\circ}$C is called R_0 and is chosen to be 100 Ω. This is to provide comparability to commercial PT100-sensors and to obtain measurable voltages with a testing current of only 1 mA. With the above values for ρ, R_0 and $d = 25\,\mu$m, the result is:

$$\begin{aligned} R_0 &= \rho \cdot \frac{\ell}{A} = \rho \cdot \frac{\ell}{\pi \cdot r^2} \qquad (2.1) \\ \Rightarrow \ell &= \frac{R_0 \cdot \pi \cdot r^2}{110 \times 10^{-9}\,\Omega\mathrm{m}} \approx 0.45\,\mathrm{m} \end{aligned}$$

Thus, one has to apply 50 cm of platinum wire on the Kapton film quite compactly. Small deviations in the order of centimeters are no problem, because each sensor has to be singly calibrated anyway. A similar wire length is desirable to allow a similar load of the current sources as well as noise filtering (more on this subject in subsequent chapters).
In principle, a platinum wire passed by an electric current is nothing else than a small ohmic heater. At $-25\,^{\circ}$C we obtain for the dissipated power a value of

$$\begin{aligned} P &= R \cdot I^2 \\ &\approx 90\,\Omega \cdot \left(1 \cdot 10^{-3}\,\mathrm{A}\right)^2 = 0.09\,\mathrm{mW} \qquad (2.2) \end{aligned}$$

According to [Kl], the error due to self-heating of a 100 Ω sensor at a current of 1 mA is 0.004 K; so with equation (2.2) we get a temperature change of about 0.0036 K at a temperature of $-25\,^{\circ}$C.

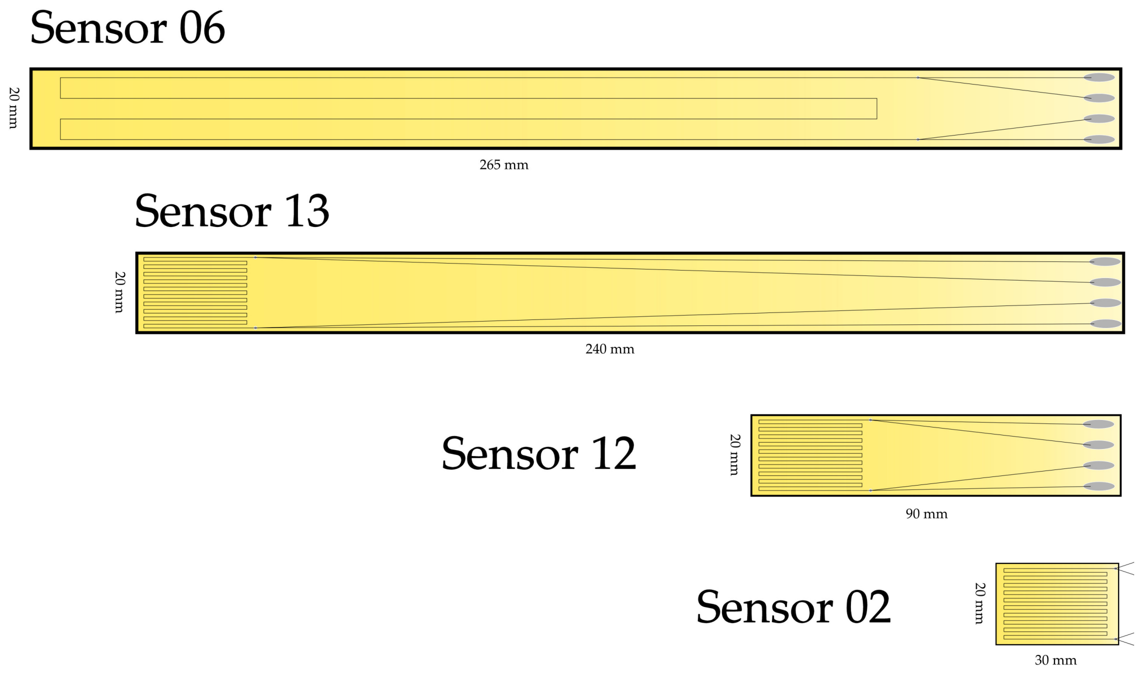

Figure 2.1: Different designs of the platinum sensors

Therefore, the rather small testing current of 1 mA seems to be well chosen and the influence of self-heating needs not be taken into account.
Different sensor designs have been developed to fathom the possibilities of constructing them (fig. 2.1). All these sensors have a thickness not noticeably larger than 60 microns at their active area (the active area is the area which is inhibited by the platinum wire between the two four-wire contacts and therefore the only material that contributes to the sensor's resistance), so that it is possible to place the sensors on the long sides of the crystals. Their width is designated uniformly to 20 mm, which is based on the dimensions of the crystals' long sides.
The length of a sensor is open to trial and error. The simplest design is one that combines only few windings and long, straight paths. With such a design, it is possible to average the temperature of a crystal's long side with straight paths in approximately the length of a crystal. Looking at figure 2.1, such a sensor is number 06. Glued on it, four long platinum wire paths with a length of 190 mm each, form the resistance. Both ends of the paths are connected with two copper wire loops, which are led to the sensor's end and connected to thicker wires for testing purposes.

2.1.2 Read-out of the Temperature Sensors

As already mentioned, the temperature sensors will be read out via a four-terminal sensing. With this method four cables are attached to the sensor. Two wires provide the constant supply current of $I_{\text{ref}} = 1$ mA while one measures a voltage U_ϑ at the other two cables. The voltage is thereby in accordance with Ohm's law

$$U_\vartheta = I_{\text{ref}} \cdot R_\vartheta \qquad , \tag{2.3}$$

whereby R_ϑ is the resistance of the sensor. Figure 2.2 illustrates this method.
The four-terminal sensing allows to neglect the resistance of the wires so that one only measures the resistance of the sensor.
Within the range below 0 °C the resistance R_ϑ depends on the temperature as follows:

$$R_\vartheta = R_0 \left(1 + a \cdot T + b \cdot T^2 + c \cdot (T - 100\,^\circ\text{C}) \cdot T^3\right) \qquad . \tag{2.4}$$

For commercial PT100 the coefficients of this equation are as follows: $a = 3.91 \cdot 10^{-3} / {}^\circ\text{C}$, $b = -5.78 \cdot 10^{-7} / {}^\circ\text{C}^2$ and $c = -4.18 \cdot 10^{-12} / {}^\circ\text{C}^4$. To reach the aspired resolution of 0.05 K the self-constructed temperature sensors must be calibrated to evaluate the above-named coefficients. By

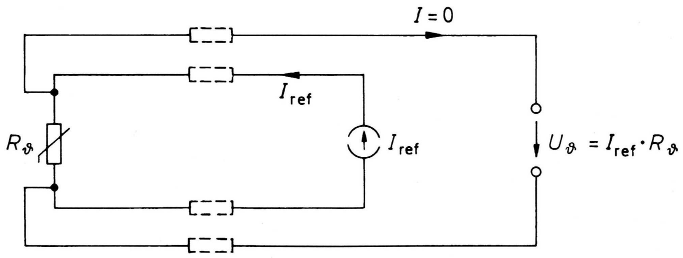

Figure 2.2: Principle of the four-terminal sensing [Ti02]

means of the two equations (2.3) and (2.4) one can obtain the temperature T of the environment. For this method it is important that the drift of the current is less than the resolution, which has to be measured.

2.2 The Humidity Sensors

For the humidity monitoring, the HIH-4000 series from Honeywell [Ho08] is selected. This sensor is a laser trimmed, thermoset polymer capacitive sensing element with an on-chip integrated signal conditioning. Thus, the output voltage of this sensor is proportional to the relative humidity (RH) and ranges from 0.8 V to 3.8 V.

Figure 2.3: HIH-4000 series. Pins from left to right: GND, OUT and V_{CC}

The sensing element's multilayer construction provides a resistance to most application hazards such as wetting, dust, dirt, oils and common environmental chemicals. With a supply voltage of +5 V DC and a typical current draw of only 200 μA, which results in 1 mW dissipated power, the HIH-4000 series is suitable for the cooled area inside the EMC. Moreover, this sensor is quite small. Without the pins, the dimensions of this sensor are only $(4.17 \times 8.59 \times 2.03)$ mm^3. Another advantage is the sensor's operating range, which goes down to $-40\,^\circ$C and 0% RH with a resonable accuracy of 3.5% RH [Ho08].
Other humidity sensors were tested but this type provides the best accuracy and performance. A precise description with several studies of the sensor's behavior can be found in ref. [Fr09].

3 Design of the THM$\overline{\mathsf{P}}$

3.1 Environmental Requirements

If the THM$\overline{\mathsf{P}}$ is placed inside the cooled area of the forward endcap, it has to fulfill the following conditions: First of all the THM$\overline{\mathsf{P}}$ must work inside a $-25\,^{\circ}$C environment without any variation from working at room temperature (RT). Second, it has to work properly in a magnetic field. According to fig. 3.1 the field strengh behind the mountplate is 1.3 T. For the Barrel part of the EMC the field strengh is even 2.5 T.

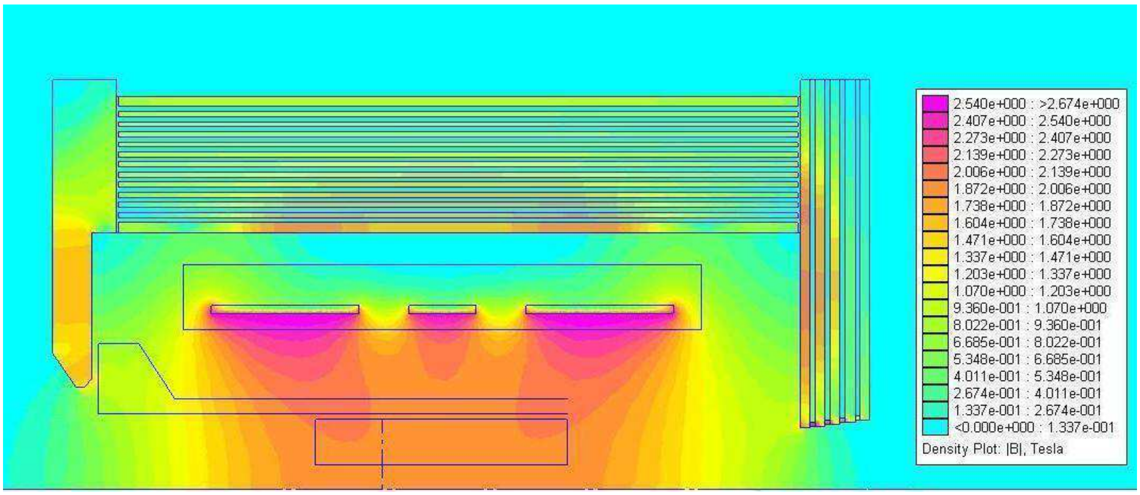

Figure 3.1: Magnetic flux density distribution of the $\overline{\mathsf{P}}$ANDA Solenoid (cross section for half of the horizontal plane where the beam comes from the left). The iron yoke, coil and cryostat, the barrel DIRC and the outer tracker are indicated by their outlines [PA09]

Third, the THM$\overline{\mathsf{P}}$ has to be radiation hard. Simulations have shown that the THM$\overline{\mathsf{P}}$ will be exposed to up to 10 mGy/h if placed behind the mountplate and the innermost crystals of the forward endcap [Ro09]. This means that in 10 years the THM$\overline{\mathsf{P}}$ will be exposed to a dose of up to 440 Gy. The PCB should at least withstand this dose without showing any significant defects due to radiation damage.

3.2 Basic Design of the THM$\overline{\mathsf{P}}$

The Temperature and Humidity Monitoring Board for $\overline{\mathsf{P}}$ANDA is designed to read out 64 channels. As described in chapter 2, the sensors differ in their supply needs and in their processing of data. In order to be flexible with the number of temperature and humidity sensors, the THM$\overline{\mathsf{P}}$ is conceived as a mainboard with connectors to eight piggyback boards. Eight sensors are connected to each piggyback board.
With this design further types of piggypack boards can be produced to monitor other signals.
Figure 3.2 shows a simplified block diagram of the THM$\overline{\mathsf{P}}$. On the mainboard an ADC and a microcontroller (MC) are attached. The data from the THM$\overline{\mathsf{P}}$ is transmitted via a CAN bus to the slow control.

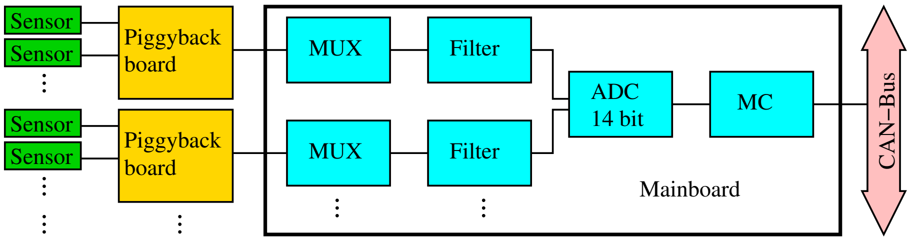

Figure 3.2: Block diagram of the THM$\overline{\text{P}}$

The temperature piggyback board is composed of current sources for the sensors and amplifiers. Due to the low current of 1 mA and the resistance of the PT100, the output voltage of these sensors varies between nearly 88.2 mV and 111.7 mV for a temperature range of −30 °C to 30 °C. However, the ADC on the mainboard has a range of 0 to 4 V. This is why the voltage is amplified. For the HIH-4000 humidity sensors only a +5 V DC supply is needed. Due to the output voltage range of these sensors no amplification is necessary.
The overall dimensions of the THM$\overline{\text{P}}$ are $(120 \times 130 \times 14)$ mm^3. A steel case reducing RF noise and facilitating mounting in the EMC will be developed.

3.3 Common Parts

The board itself is supplied with ±6 V DC. On the boards (mainboard as well as piggyback boards) low dropout voltage regulators provide the voltages needed by the ICs (c.f. fig. 3.3).

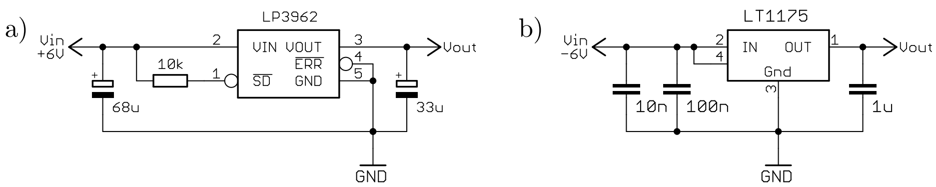

Figure 3.3: Operating circuit of the voltage regulators for the positive (a) and negative (b) voltage regulators. For the THM$\overline{\text{P}}$ +5 V, +3.3 V, and −5 V regulators will be used.

Altogether, three different voltages are required for the components of the THM$\overline{\text{P}}$. The mainboard needs a +5 V and a +3.3 V supply, the humidity piggyback board only +5 V and the temperature board needs +5 V, +3.3 V and −5 V. For the power supply and data transfer S-ATA connectors are used. The board-to-board connectors with 64 pins are from the FTE and CLE series by Samtec.

Table 3.1: Pin assignment of the connectors

SATA power		SATA data		board-to-board	
1 - 3	DGND	1, 2, 6, 7	N.C.	odd pin number	AGND
4 - 6	+6 V	3	CAN L	6, 60	AGND
7 - 9	AGND	4	DGND	2, 4	+6 V
10 - 12	−6 V	5	CAN H	62, 64	−6 V
13 - 15	AGND			12, 18, 24, 30, 42, 48, 54	signals
				others	N.C.

3.4 Mainboard

3.4.1 Multiplexer and Filter

Since the THM$\overline{\text{P}}$ has 64 channels, but the ADC just 8, the signals have to be multiplexed. Moreover, the signals have to be filtered to reduce the noise. Thus a 8:1 multiplexer MAX4581 [Ma07b] is placed next to each board-to-board connector to connect one of the eight channels of each piggyback board to the ADC. Using the microcontroller, the appropriate channels can be set up. Between the multiplexers and the ADC, 3rd order active low pass filters, such as shown in figure 3.4, are placed.

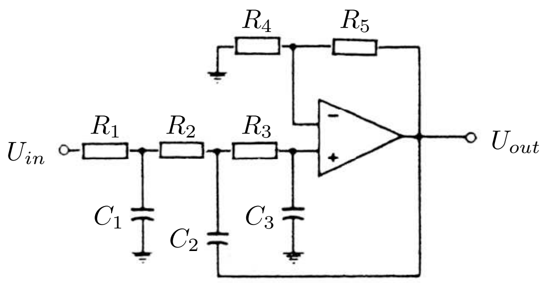

Figure 3.4: 3rd order active low pass filter [La94]

Due to the magnetic field one cannot use a passive filter with an order higher than one, because it needs inductors. On the one hand, a test measurement with a frequency synthesizer showed that a 1st order passive filter is insufficient for noise reduction. On the other hand, one wants to have as few active parts as possible to keep the heat production of the whole THM$\overline{\text{P}}$ as low as possible. If one considers that the number of operational amplifiers normally corresponds to the order of a standard active filter, the filter presented in above figure seems to be a good compromise.
It must be pointed out that R_4 works as a potential divider and thus causes an amplification of the signal. For this reason this resistor is not mounted in the filters on the THM$\overline{\text{P}}$. The other values are chosen in such a way that the cut-off-frequency of the filter is 15 Hz.

3.4.2 The Analog-to-Digital Converter

To convert the analog signals from the sensors the 14-bit ADC MAX1148 from Maxim Integrated Products, Inc. is used. The MAX1148 is a low-power, 8-channel ADC which operates from a single +4.75 V to +5.25 V supply. All analog inputs are software configurable for unipolar or bipolar and single-ended or differential operation. This ADC has an internal reference of $V_{\text{ref,i}} = 4.096$ V and a dynamic range of 0 V$\ldots V_{\text{ref}}$. The MAX1148 is built in a 20-pin TSSOP package and has a 4-wire serial interface available, which directly connects to SPI devices. It provides two clock modes to perform the analog-to-digital conversions: the internal clock mode and an external serial-interface clock respectively [Ma07a]. For SPI one has to take account of the correct clock polarity and sampling edge in the SPI control registers. To start the conversion a control byte has to be sent via the SPI (tab. 3.2). Therefore one requires three 8-bit transfers to perform a conversion. One to configure the ADC and two more to clock out the 14-bit conversion result. For the THM$\overline{\text{P}}$ the internal clock mode is used to perform the conversion. In this mode SSTRB goes low at the start of the conversion and then goes high when the conversion is complete. To reduce noise, the serial clock stays low while SSTRB is low. With an input range equal to the fullscale range of the ADC, the effective number of bits (ENOB) is 13. Furthermore, this ADC has a sampling rate of 60 ksps.

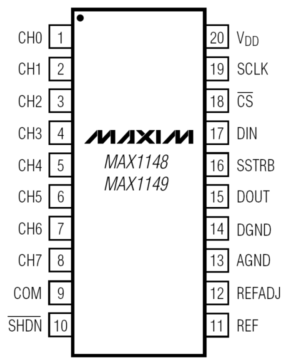

Figure 3.5: Pin configuration of the MAX1148 [Ma07a]

Table 3.2: Control byte format of the MAX1148 [Ma07a]

Bit	Name	Description
7	Start	The first logic 1 after $\overline{\text{CS}}$ goes low defines the beginning of the control byte
6 5 4	SEL2 SEL1 SEL0	Channel-select bits c.f. [Ma07a]
3	SGL/DIF	Selects single-ended (1) or differential (0) conversions
2	UNI/BIP	Selects unipolar (1) or bipolar (0) conversion mode
1 0	PD1 PD0	Selects clock and power down modes. PD1 = 0 and PD0 = 0 selects full power-down mode PD1 = 0 and PD0 = 1 selects fast power-down mode PD1 = 1 and PD0 = 0 selects internal clock mode PD1 = 1 and PD0 = 1 selects external clock mode

3.4.3 The Microcontroller

The converted data from the ADC has to be read out and sent to the slow-control to monitor the temperature and humidity inside the detector. For the first task a device with SPI is required, for the second task a CAN-Bus is to be used. Therefore the AT90CAN64 from Atmel Corporation [At08a], an 8-bit AVR microcontroller with 64 kB ISP flash and CAN controller, has been selected. Using the STK500 development system from Atmel, the MC can be programmed via an RS232 interface. This development board is connected to the mainboard over a AVR-ISP interface, which is described in [At08b, Fe09]. To be able to be responsive to bugs and potential changes for the monitoring it is planned to flash a CAN bootloader on the microcontroller according to [At05].
To read out the ADC the SPI clock is set to 125 kHz and the control byte is set to $1XXX1110$, whereby XXX stands for the appropriate channel selection. Figure 3.6 shows a transfer between the ADC and the microcontroller.

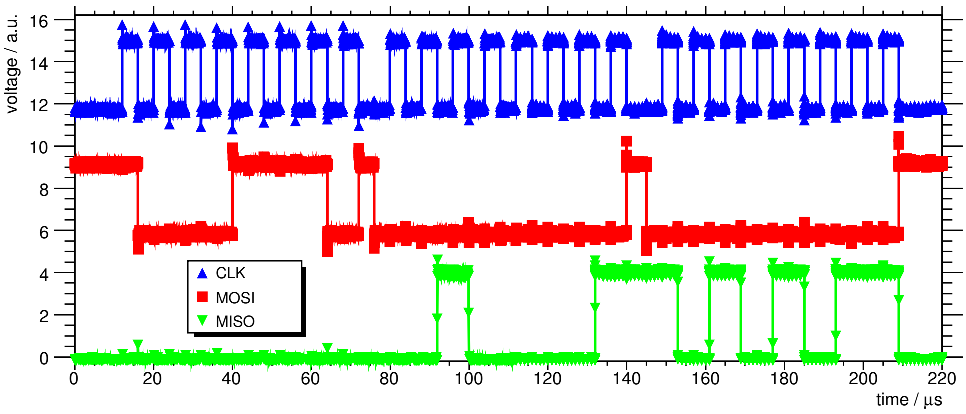

Figure 3.6: Complete SPI transfer between the AT90CAN64 and the MAX1148. For a better view the values of CLK and MOSI are shifted.

For a better view of the individual signals, the clock and MOSI signals were shifted in this plot. One can clearly see the three bytes transferred, the control byte and two bytes with the converted data. It is planned to measure each signal several times and average them to reduce the uncertainty before transmitting the data via the CAN bus.

3.5 Piggyback Board for the Humidity Sensors

The humidity sensors were already described in chapter 2.2. As mentioned in that chapter they only need a +5 V power supply. The output voltage uses nearly the full range of the ADC so that no amplification of the signals is required. Therefore this PCB only consists of a voltage regulator as shown in figure 3.3a) and eight fuses. The fuses prevent a short-circuit of the humidity sensors due to radiation damage.

3.6 Piggyback Board for the Temperature Sensors

The main part of this board is the current source for the sensors. Different types of current sources were developed and tested. The results of these tests will be presented in the next chapter of this report. The instrumentation amplifier AD623 [AD08a] is used for amplification of the signals. This amplifier has an adjustable gain G, which can be set up with a resistor R_G between the pins 1 and 8 according to

$$G = 1 + \frac{100\,\mathrm{k}\Omega}{R_G} \quad . \tag{3.1}$$

It is also possible to put an offset on the signal. The amplifier itself is symmetrically supplied with ±5 V DC. It was planned to amplify the signal by a factor of nearly 70 and subtract an offset of 5 V so that one ends up with a signal range of roughly 1.2 to 2.8 V instead of 88 to 112 mV. According to fig. 3.7 unfortunately this is not possible.

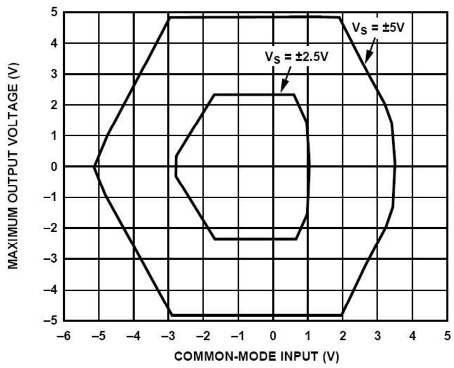

Figure 3.7: Maximum output voltage vs. common-mode input [AD08a]

Due to the design of the current source the input voltages are 2.5 and 2.6 V at 0 °C. Therefore the maximum output voltage without any offset is roughly 3.5 V. This is the reason why actually only an amplification of 30 and no offset voltage is used. This means that the signals applied to the ADC have a range of approximately 2.6 to 3.4 V. Figure 3.8 illustrates the basic design of the temperature piggyback board.

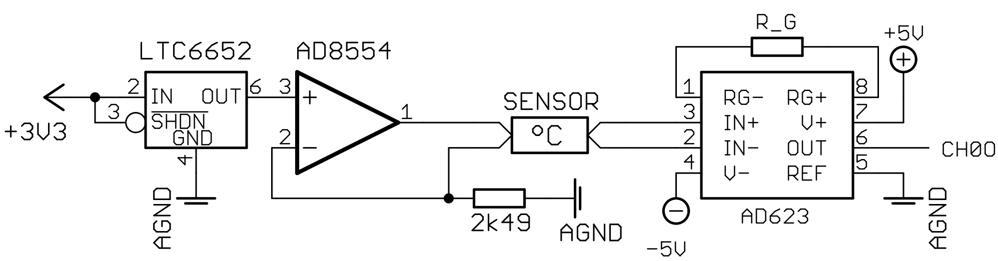

Figure 3.8: Simplified schematic of the temperature piggyback board

4 Test Measurements of the $\mathrm{TH M\overline{P}}$

4.1 Current Sources

As mentioned in chapter 2.1 the drift of the current sources should be smaller than the resolution. A measurable sensitivity of 0.05 K, which corresponds to a change of the light yield of 0.15%, is aimed for. This accords with a change of the resistance of the sensor of 0.02 Ω. Therefore the current drift should be smaller than $2 \cdot 10^{-4}$ / 0.05 K.
Overall, three different types of current sources with different variants were tested. In a climatic chamber the temperature dependencies of the sensor current were measured between −30 °C and +30 °C.

4.1.1 Design Descriptions

Figure 4.1 shows the schematics of the three types of current sources.

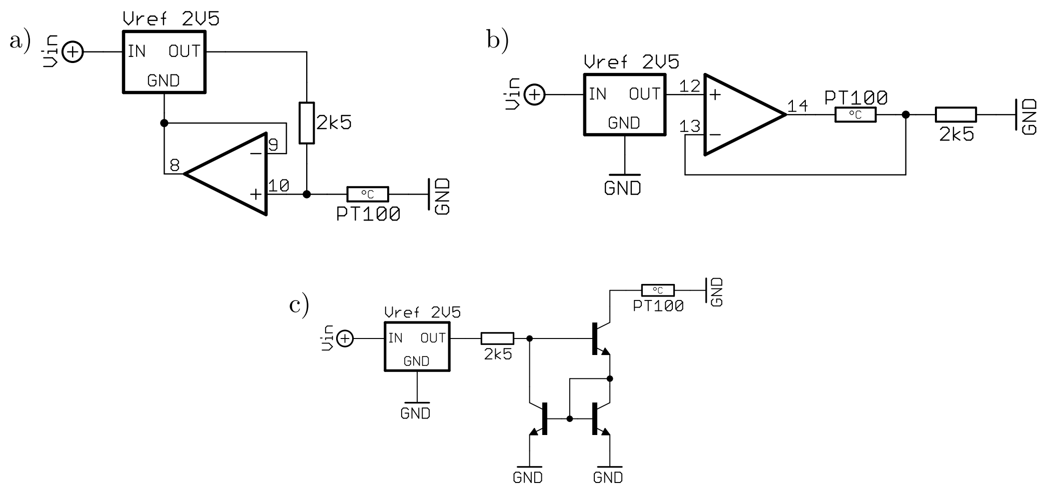

Figure 4.1: The three tested versions of the current source

The first version consists of a 2.5 V reference, a 2.5 kΩ precision resistor and an operational amplifier. During development, attention was focused on the temperature drift of these devices. This source was developed and tested with different parts. For the voltage reference the ADR441 from Analog Devices [AD08c] and the LTC6652 from Linear Technology [LT08b] were used, and for the operational amplifier the OPA4241 and the AD8554 from Analog Devices [AD08b] were used. The voltage drops across the 2.5 kΩ resistance to provide the needed current of 1 mA. The current is applied to the temperature sensor as well as to the non-inverting input of the amplifier, whose output is attached to the virtual ground of the reference and the inverting input. This circuit stabilizes the reference and is self-adjusting.
The second version (fig. 4.1b) is pretty similar to the first one. The reference voltage is attached to the non-inverting input of the amplifier. The sensor has to be connected to the output and fed back to the inverting input. The advantage of this design is, that one can build multiple current sources with only one voltage reference. This design was only tested with the LTC6652 and AD8554.
The third current source is a Wilson current mirror. Like the other two versions, this one contains a 2.5 V reference and a high precision 2.5 kΩ resistor to provide the current of 1 mA. According to literature (e.g. [Ti02]), this current mirror is a very stable current source.

4.1.2 Test Results

To study the temperature drift of the sources each developed version was operated in a climatic chamber. The sensor current was measured every 20 seconds with the Agilent 34980A digital multimeter [Ag09]. Per test measurement, 61 temperature values from $-30\,°\text{C}$ to $+30\,°\text{C}$, were recorded with a step size of one degree Celsius at intervals of one hour. This means that 180 values are measured per temperature step. Due to temperature variation caused by control hysteresis of the climatic chamber and not yet constant temperatures of the ICs, the first 30 values were not taken into account. The remaining values were filled into a histogram and a Gauß distribution was fitted to them. The mean of the distribution is plotted against the respective temperature. Figure 4.2 shows the results of these measurements. Since the versions with the ADR441 and the OPA4241 delivered nonsatisfying results, they are not considered here.

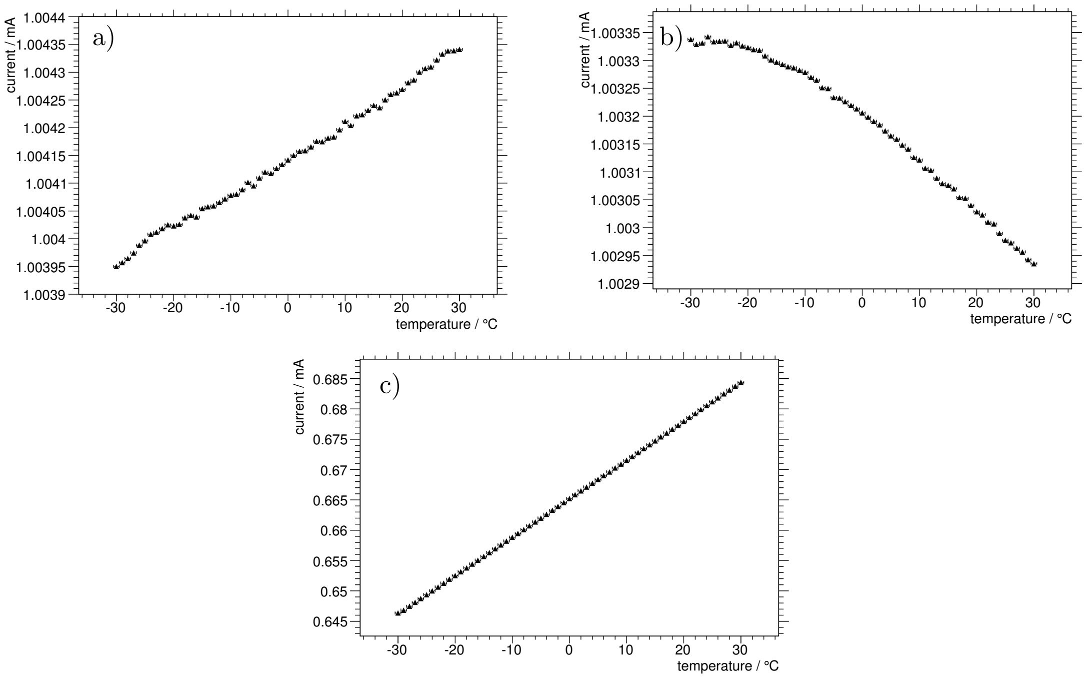

Figure 4.2: Sensor current vs temperature

Contrary to expectations the Wilson current mirror has the largest drift with $7 \cdot 10^{-4}$ mA/K. Also the sensor current drift of this source is lower than was requested (cf fig. 4.2c). The first and second versions show a drift of roughly $2 \cdot 10^{-5}$ mA/K (fig. 4.2a and b). Regarding the operational point at $T = -25\,°\text{C}$ version 2 has nearly a constant current output. Therefore this version which consists of fewer parts, will be used for the THM$\overline{\text{P}}$. It remains to be said that this version was tested with a precision resistor, which has a temperature drift of only 0.2 ppm/K, and a 2.49 kΩ resistor with 10 ppm/K. No significant difference in the behavior of the source has been observed during the measurements, neither with the high precision resistor nor with the one with 10 ppm/K. Therefore, the resistor with 10 ppm/K is being used.

4.2 Temperature Cycles

One aim of development was the proper operation of the THM$\overline{\text{P}}$ in a temperature range from $-30\,°\text{C}$ to $+30\,°\text{C}$. In order to check this, a prototype of the THM$\overline{\text{P}}$ was installed in the climatic chamber. One humidity and one temperature piggyback board were attached to the mainboard, each with two sensors. For evaluating the self-constructed temperature sensors a commercial PT100 was used as second sensor. Analogous to the tests of the current sources, 61 temperature steps at an intervall of one hour each, were measured. The data from the ADC was read out with an AVR32ngw100

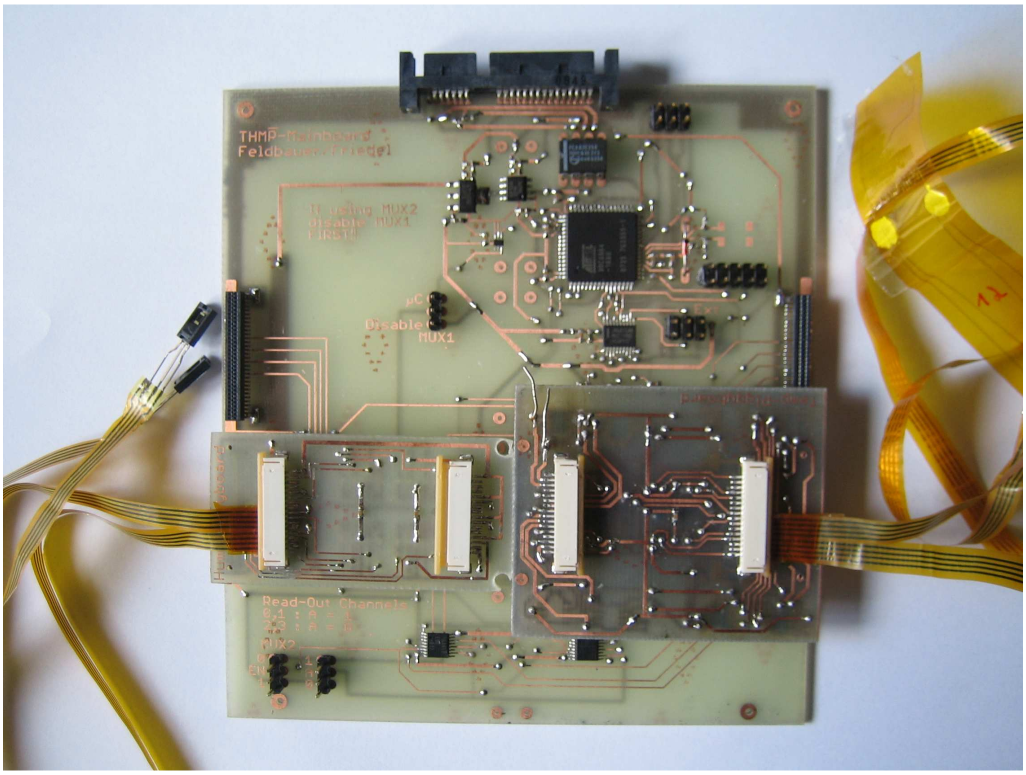

Figure 4.3: Prototype of the THM$\overline{\text{P}}$. The figure shows the mainboard with one humidity and one temperature piggyback board attached.

from Atmel. Nothing unusual was noted in these measurements; for further information please refer to [Fr09].

4.3 Measurements in a Magnetic Field

In case the THM$\overline{\text{P}}$ is placed inside the cooled area of the EMC it has to work properly in a magnetic field of 1.3 T for the endcap and 2.5 T for the barrel part. First tests with the aforesaid prototype were carried out in a magnetic field of 1.5 T. In figure 4.4 the measured values are plotted against the time. During the first four minutes, in which the magnetic field increases from 0 to 1.5 T, no effects were observed.

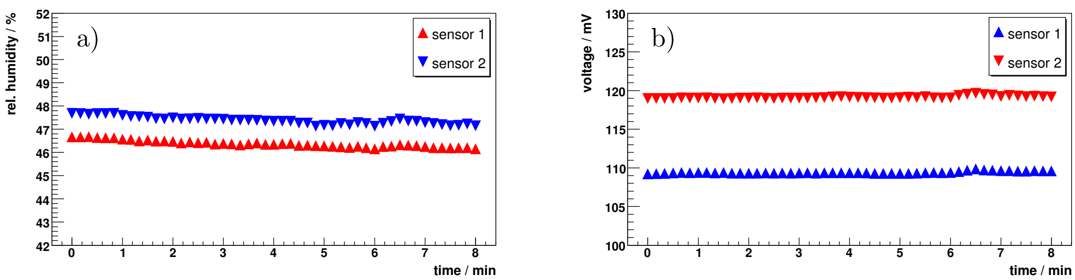

Figure 4.4: Temporal development of the sensor output in a magnetic field. a) measured RH of two humidity sensors, b) measured voltage output of two temperature sensors.

In the following three minutes, the angle between the magnetic field and the THM$\overline{\text{P}}$ including the sensors was varied between 0° and 90°, and in the last minute the magnetic field was shut down. The small decrease of the RH and the increase of the temperature respectively, are caused by the heating-up of the magnet. As no unexpected effects appeared during this test, one can assume that the THM$\overline{\text{P}}$ will work in a magnetic field of up to 1.5 T. However, the behavior of the THM$\overline{\text{P}}$ remains to be tested in a magnetic field of 2.5 T and also if the magnet quenches.

4.4 Studies of Radiation Hardness

The irradiation tests were carried out at Gießen Irradiation Facility, where the THM$\overline{\text{P}}$ was irradiated with a ^{60}Co-source, which emits two photons with an energy of 1.17 and 1.33 MeV by its decay. The source has an activity of 10^{13} Bq, thus a rate of about 210 Gy/h at a distance of 20 cm can be achieved [No09]. This rate is by far higher than the highest dose expected in the $\overline{\text{P}}$ANDA detector. Like for the measurements in the magnetic field, two sensors were attached to each piggyback board and the ADC was read out every second with the AVR32ngw100. In the first test, the THM$\overline{\text{P}}$ was exposed to 660 Gy. The signals of the humidity sensors linearly increased immediately after starting the irradiation, while the voltage output of the temperature sensors remaind nearly constant. Approximately after 1.75 h the signals of all four sensors began to rise exponentially until they reached the overflow of the ADC. The output voltage of the temperature sensors broke down after 2.7 h, which led to the assumption that one or more parts were not radiation-hard. When measuring the voltages on the PCB it turned out, that the used voltage regulator MIC5200 from Micrel [Mi05] was damaged and put through the supply voltage of 6 V DC. Further tests showed that the output voltage rose linearly with the accumulated dose until it reached the supply voltage.The observed effects can be explained by the changing supply voltage [Fr09].
For a second test, in which nearly 500 Gy were accumulated, the voltage regulator LT1129 [LT08a] was used and withstood the radiation. However, the -5 V DC regulators of type LT1175 [LT05] were destroyed, but the exact dose was not monitored. This is why more tests will be done to determine the upper limit of the radiation dose the parts can withstand.
In a third radiation test another positive voltage regulator was irradiated. A total dose of 720 Gy was accumulated in the LP3962 from National Semiconductor [Na06]. No changes during or after the irradiation could be observed, so that this type of positive voltage regulator will be used for the THM$\overline{\text{P}}$. This regulator is also employed by the GSI for the ASICs [Wi09].
Further tests were carried out and showed that the HIH-4000 humidity sensor are radiation-hard up to 530 Gy.

Table 4.1: Maximum tested dose for each part it withstood at a rate of 210 Gy/h

part	description	dose [Gy]
MIC5200[1]	positive low drop-out regulator	~ 0
LT1129[1]	positive low drop-out regulator	> 500
LP3962	positive low drop-out regulator	> 720
LT1175[2]	negative low drop-out regulator	~ 680
LTC6652	voltage reference	> 1160
AT90CAN64	8-bit AVR MC	> 720
MAX1148	14-bit ADC	> 1160
MAX4581	8:1 MUX	> 1160
AD8554	quad OpAmp	> 1160
AD623	instrumentation amplifier	> 1160
PCA82C250	CAN transceiver	> 1160
HIH-4000	humidity sensor	~ 530
self-constructed PT100	temperature sensor	> 1160

[1]No longer in use.
[2]The radiation hardness of this device will be tested again.

5 Summary and Outlook

The THM$\overline{\text{P}}$ was developed for monitoring the temperature and humidity inside the EMC. Therefore, proper operation in the cooled area has to be guaranteed. Different tests were done to ensure that the THM$\overline{\text{P}}$ works reliably in this environment.
The radiation hardness of all components was tested with a dose of at least 720 Gy. The temperature dependencies of the individual parts are beneath their critical limits. The proper operation in a magnetic field of up to 1.5 T is also assured.
In future, one has to check if the THM$\overline{\text{P}}$ will also work in a magnetic field of 2.5 T. Moreover, the radiation hardness of the negative voltage regulator for the THM$\overline{\text{P}}$ has to be studied in more detail. This will be done soon at Gießen Irradiation Facility. Furthermore it is considered to replace the instrumental amplifier of the temperature piggyback board to enlarge the signal range applied to the ADC.
Meanwhile two test samples of the mainboard have been produced with the final four-layer design. A first test of the whole THM$\overline{\text{P}}$ in a realistic environment will be done with the PROTO192 prototype of the forward endcap. Four to five boards will monitor the temperature and humidity inside this prototype to ensure that the cooling, insulation and nitrogen flushing are performing as expected.

ADC Analog to Digital Converter

C Capacitance

CAN Controller Area Network

CMOS Complementary Metal Oxide Semiconductor

EMC Electromagnetic Calorimeter

ENOB Effective Number of Bits

FAIR Facility for Antiproton and Ion Research

GSI Gesellschaft für Schwerionenforschung

HEP High Energy Physics

HESR High Energy Storage Ring

J-FET Junction Field-Effect Transistor

L Inductance

LED Light Emitting Diode

LY Light Yield

MC Microcontroller

MISO Master Input, Slave Output

MOSI Master Output, Slave Input

MSOP Micro Small-Outline Package

MUX Multiplexer

N.C. not connected

PANDA Pbar Annihilation at Darmstadt

PCB Printed Circuit Board

PWO Lead Tungstate

R Resistance

RH Relative Humidity

RT Room Temperature

SMD Surface-Mounted Device

SOP Small-Outline Package

SOT Small-Outline Transistor

SS Slave Select

SPI Serial Peripheral Interface

THMP Temperature and Humidity Monitoring Board for PANDA

TSSOP Thin-Shrink Small Outline Package

References

[AD08a] Analog Devices, *AD623: Single-Supply, Rail-to-Rail, Low Cost Instrumentation Amplifier*, July 2008, Datasheet.

[AD08b] Analog Devices, *AD8551/AD8552/AD8554: Zero-Drift, Single-Supply, Rail-to-Rail Input/Output Operational Amplifiers*, September 2008, Datasheet.

[AD08c] Analog Devices, *ADR440/ADR441/ADR443/ADR444/ADR445: Ultralow Noise, LDO XFET Voltage References with Current Sink and Source*, March 2008, Datasheet.

[Ag09] Agilent Technologies, *Agilent 34980A: Multifunction Switch / Measure Unit Sink and Source*, August 2009, Datasheet.

[At05] Atmel Corporation, *AVR914: CAN & UART based Bootloader for AT90CAN32, AT90CAN64 & AT90CAN128*, November 2005, Application Note.

[At08a] Atmel Corporation, *AT90CAN32, AT90CAN64 & AT90CAN128: 8-bit AVR Microcontroller with 32k/64k/128k Bytes of ISP Flash and CAN Controller*, August 2008, Datasheet.

[At08b] Atmel Corporation, *AVR042: AVR Hardware Design Considerations*, April 2008, Application Note.

[Fe09] F. Feldbauer, *Studien zur Strahlenhärte von Bleiwolframat-Kristallen*, Master's thesis, Ruhr-Universität Bochum, Institut für Experimentalphysik I, 2009.

[Fr09] P. Friedel, *Studien zum Prototypaufbau des elektromagnetischen Kalorimeters für den $\overline{\mathrm{P}}$ANDA-Detektor*, Diploma thesis, Ruhr-Universität Bochum, Institut für Experimentalphysik I, 2009.

[Ho08] Honeywell, *HIH-4000 Series Humidity Sensors*, May 2008, Datasheet.

[Kl] Klasmeier Kalibrier- und Messtechnik GmbH, *Arbeitsnormalthermometer: Platinwiderstandsthermometer*.

[La94] D. Lancaster, *Das Aktiv-Filter Kochbuch*, IWT-Verlag GmbH, 8. Auflage, 1994.

[LT05] Linear Technology, *LT1175: 500 mA Negative Low Dropout Micropower Regulator*, March 2005, Datasheet.

[LT08a] Linear Technology, *LT1129: Micropower Low Dropout Regulators with Shutdown*, December 2008, Datasheet.

[LT08b] Linear Technology, *LTC6652: Precision Low Drift Low Noise Buffered Reference*, December 2008, Datasheet.

[Ma07a] Maxim Integrated Products, Inc., *MAX1146-MAX1149: Multichannel, True-Differential, Serial, 14-Bit ADCs*, January 2007, Datasheet.

[Ma07b] Maxim Integrated Products, Inc., *MAX4581-MAX4583: Low-Voltage, CMOS Analog Multiplexers/Switches*, June 2007, Datasheet.

[Mi05] Micrel, *MIC5200: 100 mA Low-Dropout Regulator*, April 2005, Datasheet.

[Na06] National Semiconductor, *LP3962/LP3965: 1.5 A Fast Ultra Low Dropout Linear Regulators*, September 2006, Datasheet.

[No09] R. Novotny, private communication, 2009.

[PA09] W. Erni et al. (PANDA Collaboration), *Technical Design Report for: $\overline{\text{P}}$ANDA Solenoid and Dipole Spectrometer Magnets*, FAIR, February 2009.

[Ro09] B. Roth, private communication, 2009.

[Sc09] J. Schulze, *Prototypenentwicklung für das Elektromagnetische Kalorimeter des* $\overline{\mathsf{P}}\mathsf{ANDA}$ *Experimentes*, Diploma thesis, Ruhr-Universität Bochum, Institut für Experimentalphysik I, 2009.

[Ti02] U. Tietze and C. Schenk, *Halbleiter-Schaltungstechnik*, Springer-Verlag, 12. Auflage, 2002.

[Wi09] P. Wieczorek, private communication, 2009.

[Zh09] J. Zhong, private communication, 2009.

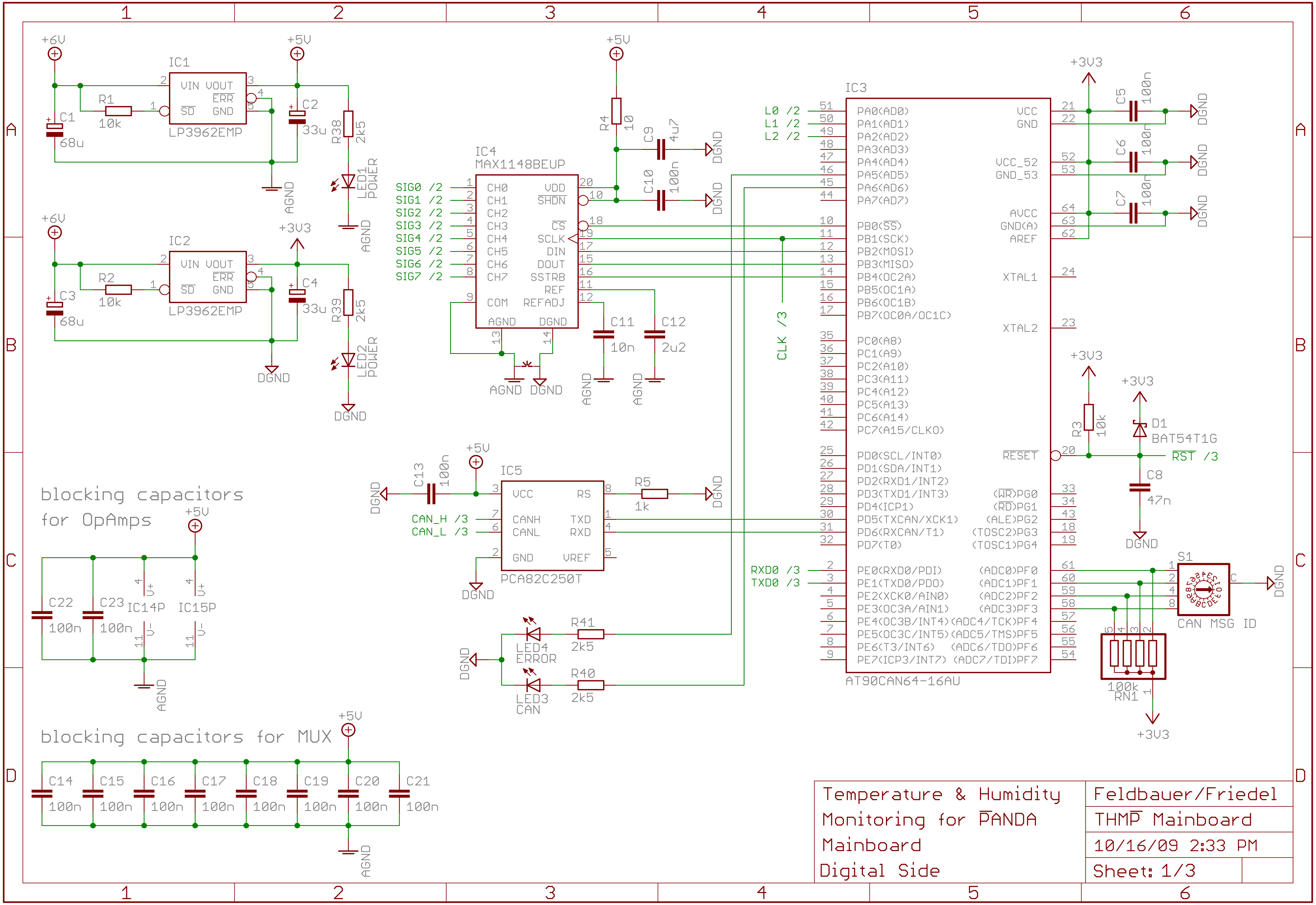

Temperature & Humidity
Monitoring for PANDA
Mainboard
Digital Side
Feldbauer/Friedel
THMP Mainboard
10/16/09 2:33 PM
Sheet: 1/3
blocking capacitors
for OpAmps
blocking capacitors for MUX
IC1
LP3962EMP
IC2
LP3962EMP
IC3
AT90CAN64-16AU
IC4
MAX1148BEUP
IC5
PCA82C250T
S1
CAN MSG ID
RN1
100k
D1
BAT54T1G
LED1
POWER
LED2
POWER
LED3
CAN
LED4
ERROR
RST /3
CLK /3
L0 /2
L1 /2
L2 /2
RXD0 /3
TXD0 /3
CAN_H /3
CAN_L /3
SIG0 /2
SIG1 /2
SIG2 /2
SIG3 /2
SIG4 /2
SIG5 /2
SIG6 /2
SIG7 /2

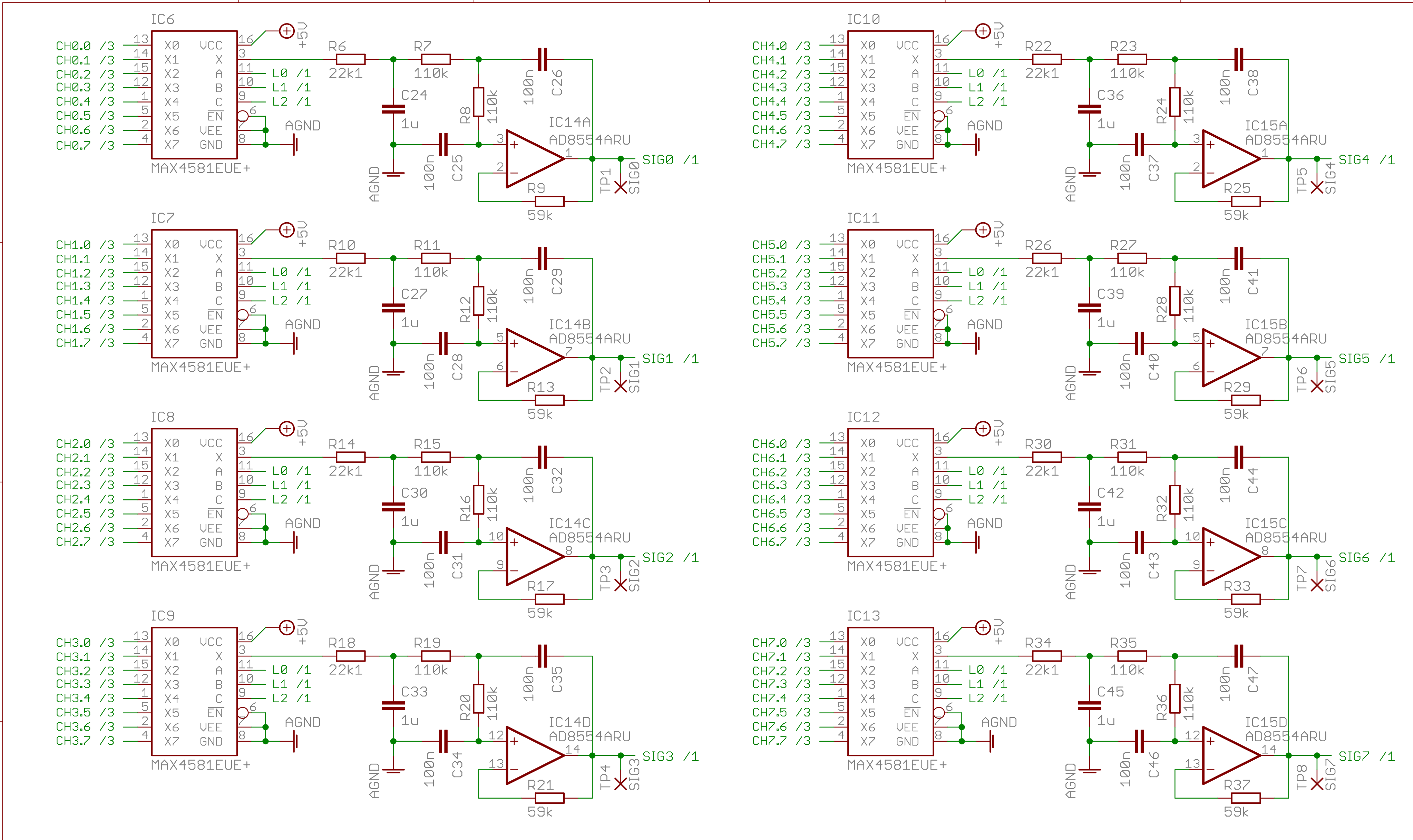

Temperature & Humidity Monitoring for PANDA Mainboard	Feldbauer/Friedel
	THMP Mainboard
	10/16/09 2:33 PM
Multiplexers and Filters	Sheet: 2/3

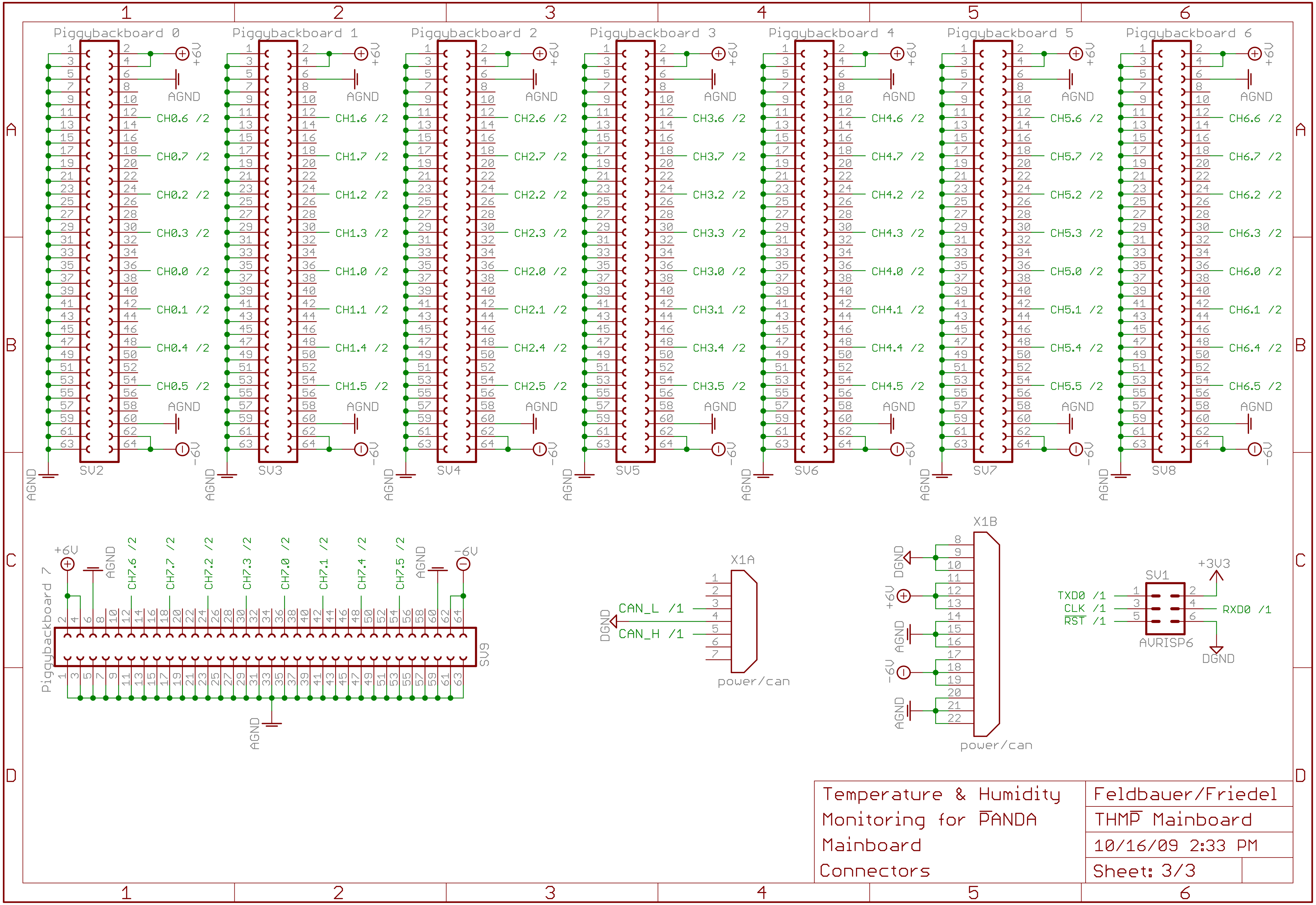

Piggybackboard 0
Piggybackboard 1
Piggybackboard 2
Piggybackboard 3
Piggybackboard 4
Piggybackboard 5
Piggybackboard 6
Piggybackboard 7
SV1
SV2
SV3
SV4
SV5
SV6
SV7
SV8
SV9
CH0.6 /2
CH0.7 /2
CH0.2 /2
CH0.3 /2
CH0.0 /2
CH0.1 /2
CH0.4 /2
CH0.5 /2
CH1.6 /2
CH1.7 /2
CH1.2 /2
CH1.3 /2
CH1.0 /2
CH1.1 /2
CH1.4 /2
CH1.5 /2
CH2.6 /2
CH2.7 /2
CH2.2 /2
CH2.3 /2
CH2.0 /2
CH2.1 /2
CH2.4 /2
CH2.5 /2
CH3.6 /2
CH3.7 /2
CH3.2 /2
CH3.3 /2
CH3.0 /2
CH3.1 /2
CH3.4 /2
CH3.5 /2
CH4.6 /2
CH4.7 /2
CH4.2 /2
CH4.3 /2
CH4.0 /2
CH4.1 /2
CH4.4 /2
CH4.5 /2
CH5.6 /2
CH5.7 /2
CH5.2 /2
CH5.3 /2
CH5.0 /2
CH5.1 /2
CH5.4 /2
CH5.5 /2
CH6.6 /2
CH6.7 /2
CH6.2 /2
CH6.3 /2
CH6.0 /2
CH6.1 /2
CH6.4 /2
CH6.5 /2
CH7.6 /2
CH7.7 /2
CH7.2 /2
CH7.3 /2
CH7.0 /2
CH7.1 /2
CH7.4 /2
CH7.5 /2
+6V
-6V
AGND
DGND
+3V3
X1A
X1B
power/can
CAN_L /1
CAN_H /1
TXD0 /1
CLK /1
RST /1
RXD0 /1
AVRISP6
Temperature & Humidity
Monitoring for PANDA
Mainboard
Connectors
Feldbauer/Friedel
THMP Mainboard
10/16/09 2:33 PM
Sheet: 3/3

Top side

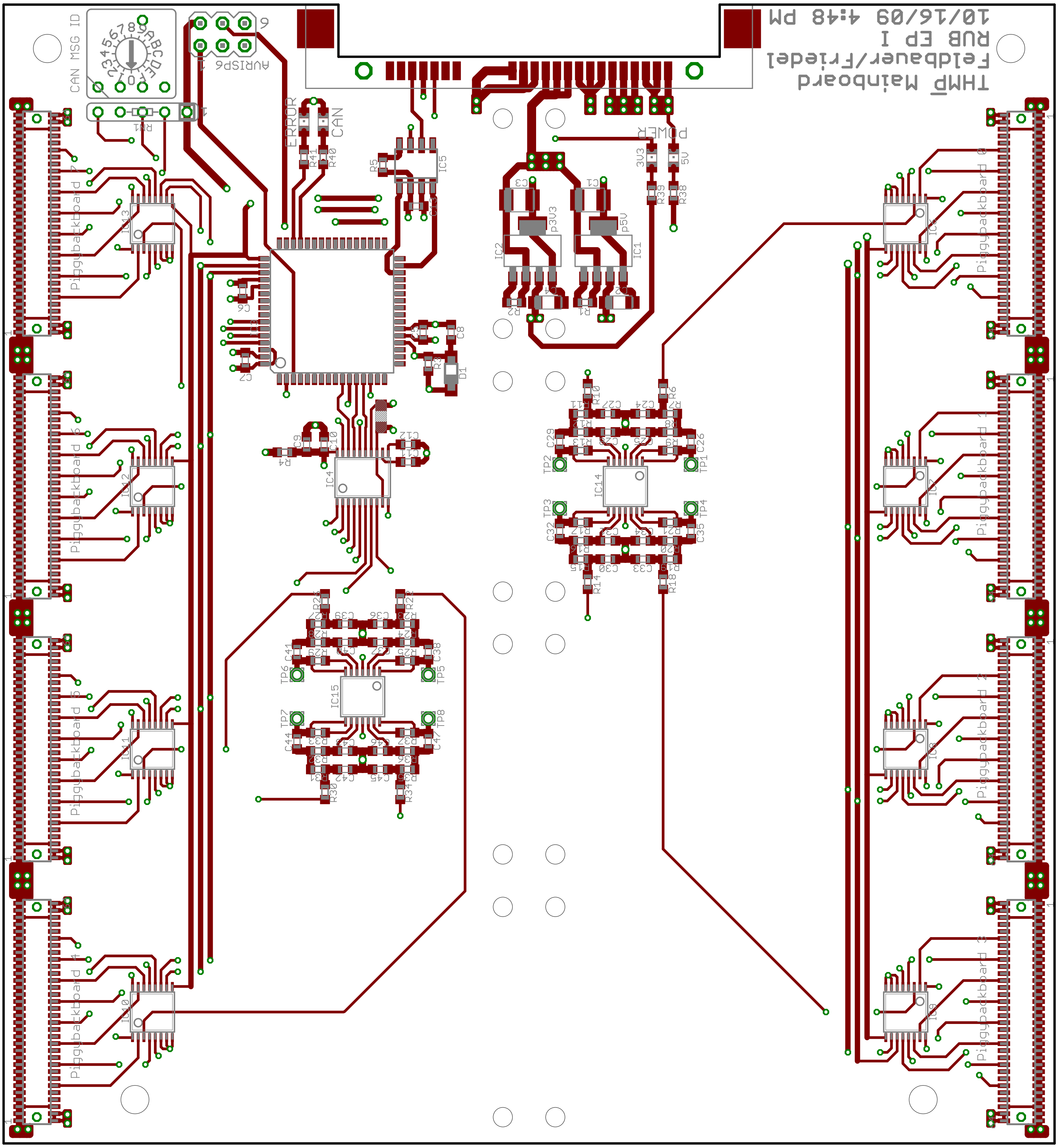
THMP Mainboard
Feldbauer/Friedel
RUB EP I
10/16/09 4:48 PM
CAN MSG ID
AVRISP6
ERROR
CAN
POWER
Piggybackboard 0
Piggybackboard 1
Piggybackboard 2
Piggybackboard 3
Piggybackboard 4
Piggybackboard 5
Piggybackboard 6
Piggybackboard 7

Bottom side

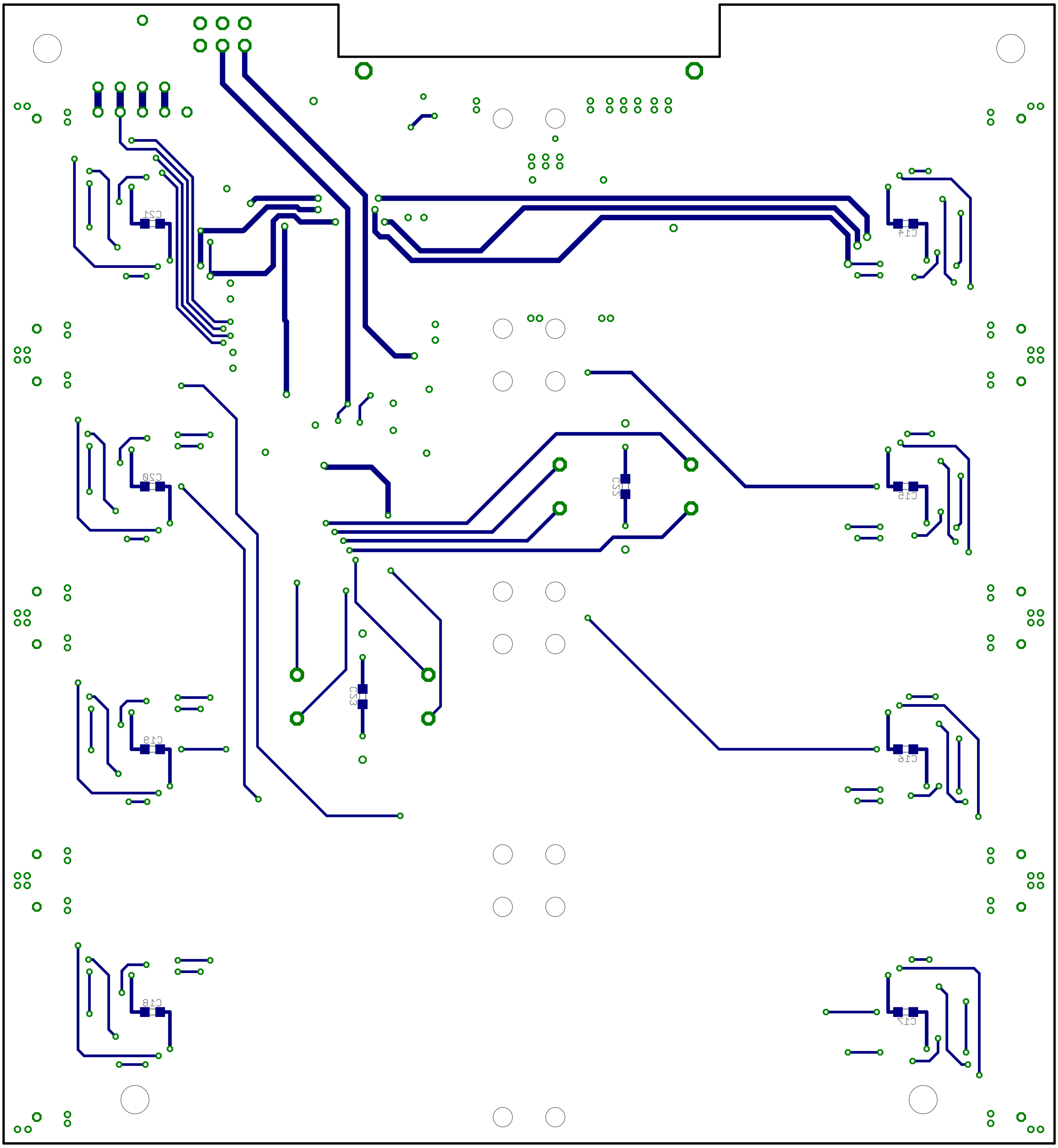

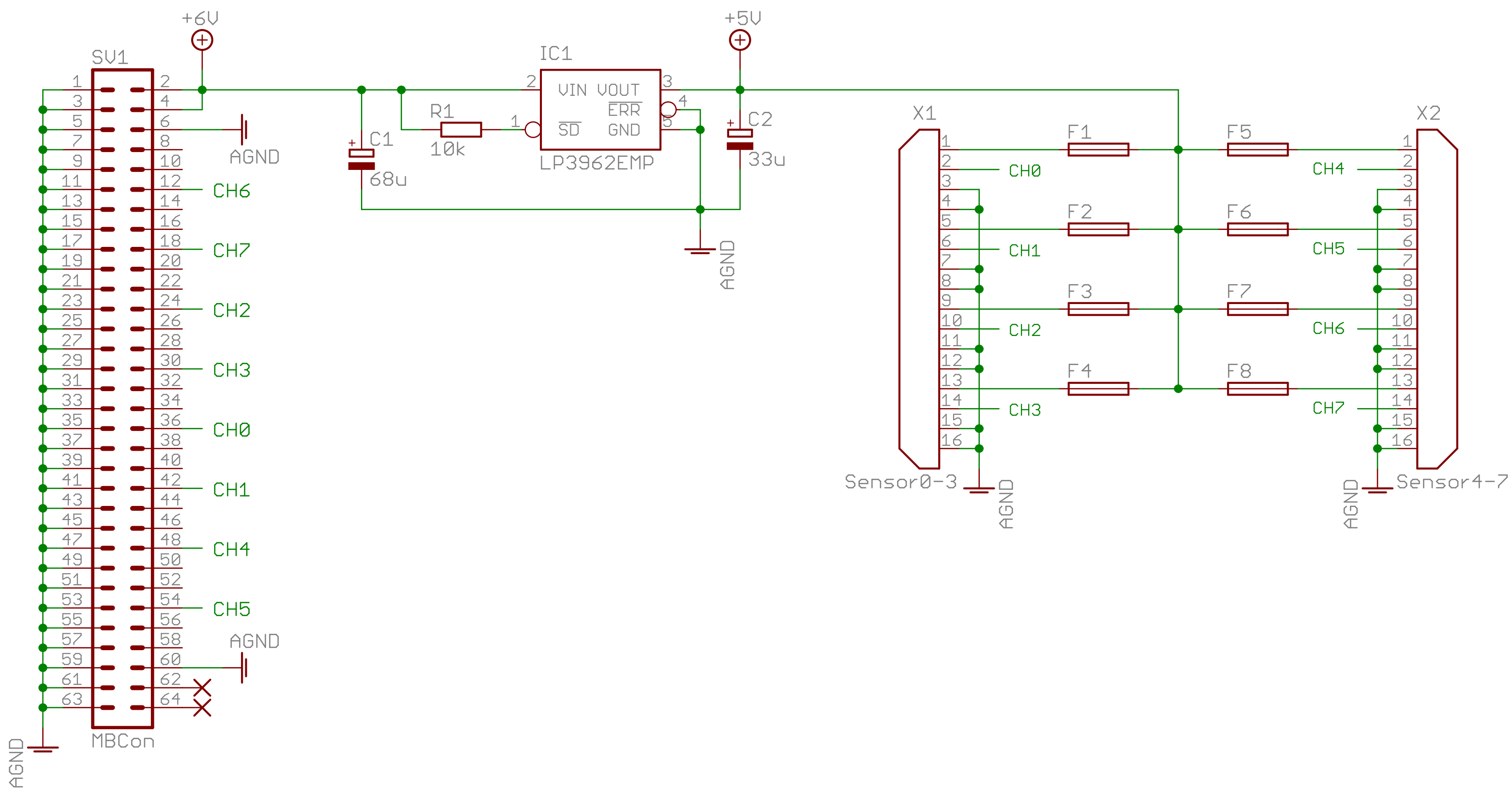

Temperature & Humidity
Monitoring for PANDA
Humidity Piggybackboard

Feldbauer/Friedel
Humidity PBB
10/8/09 1:54 PM
Sheet: 1/1

Top side

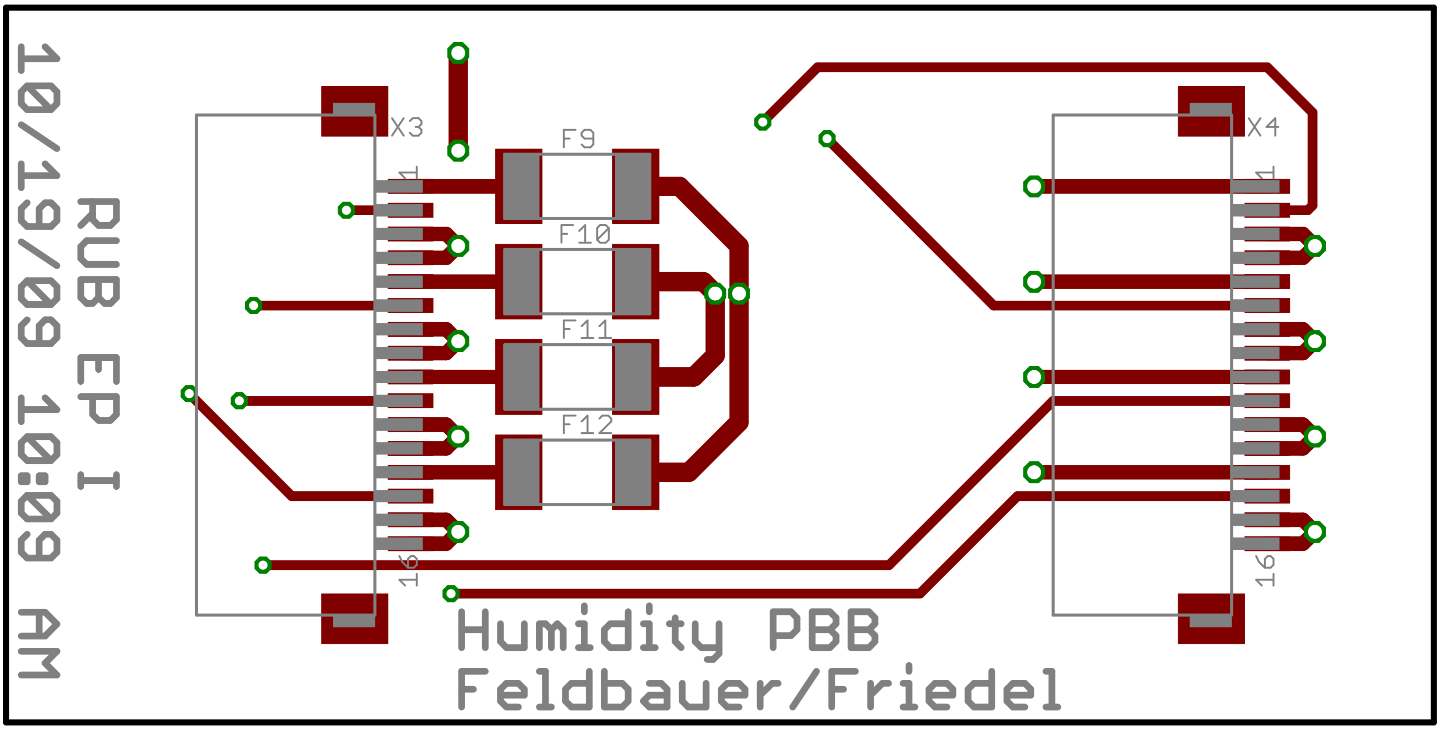

Bottom side

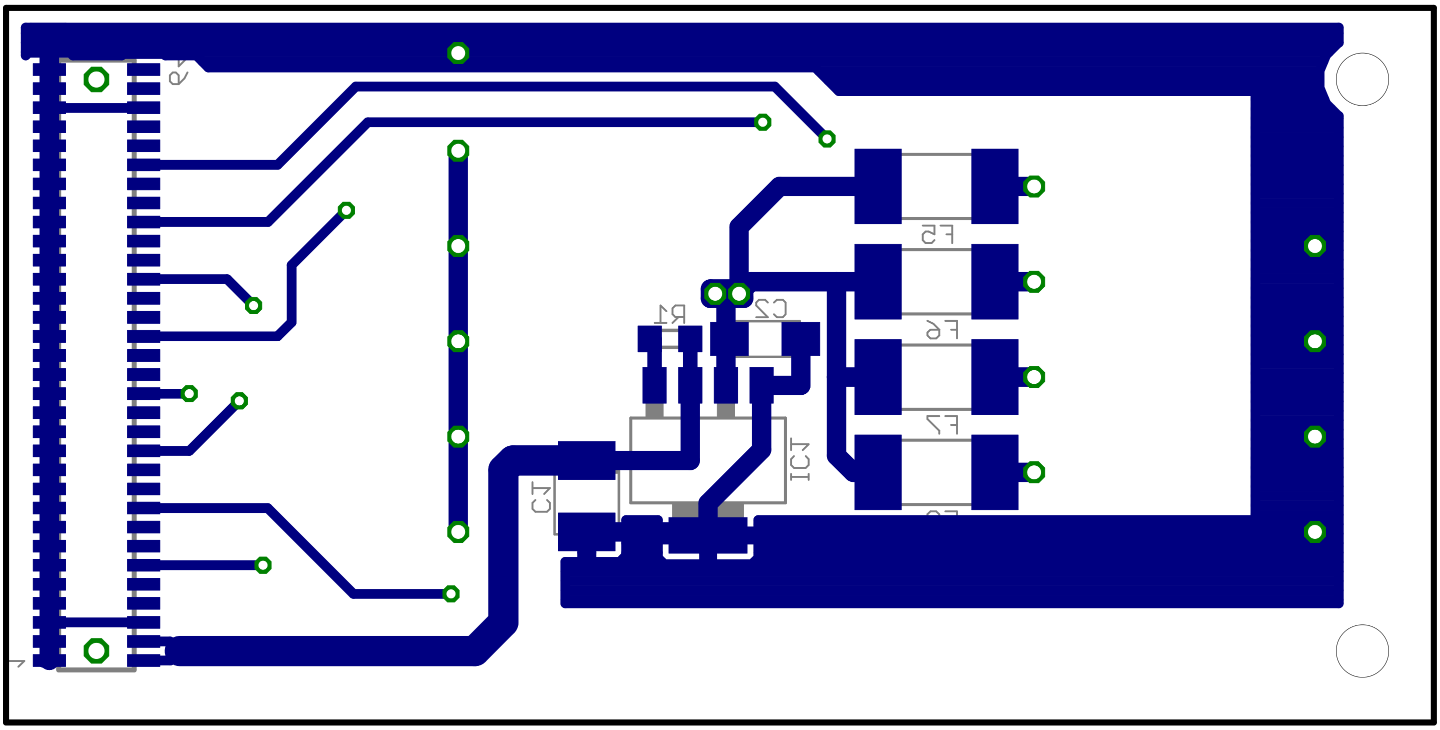

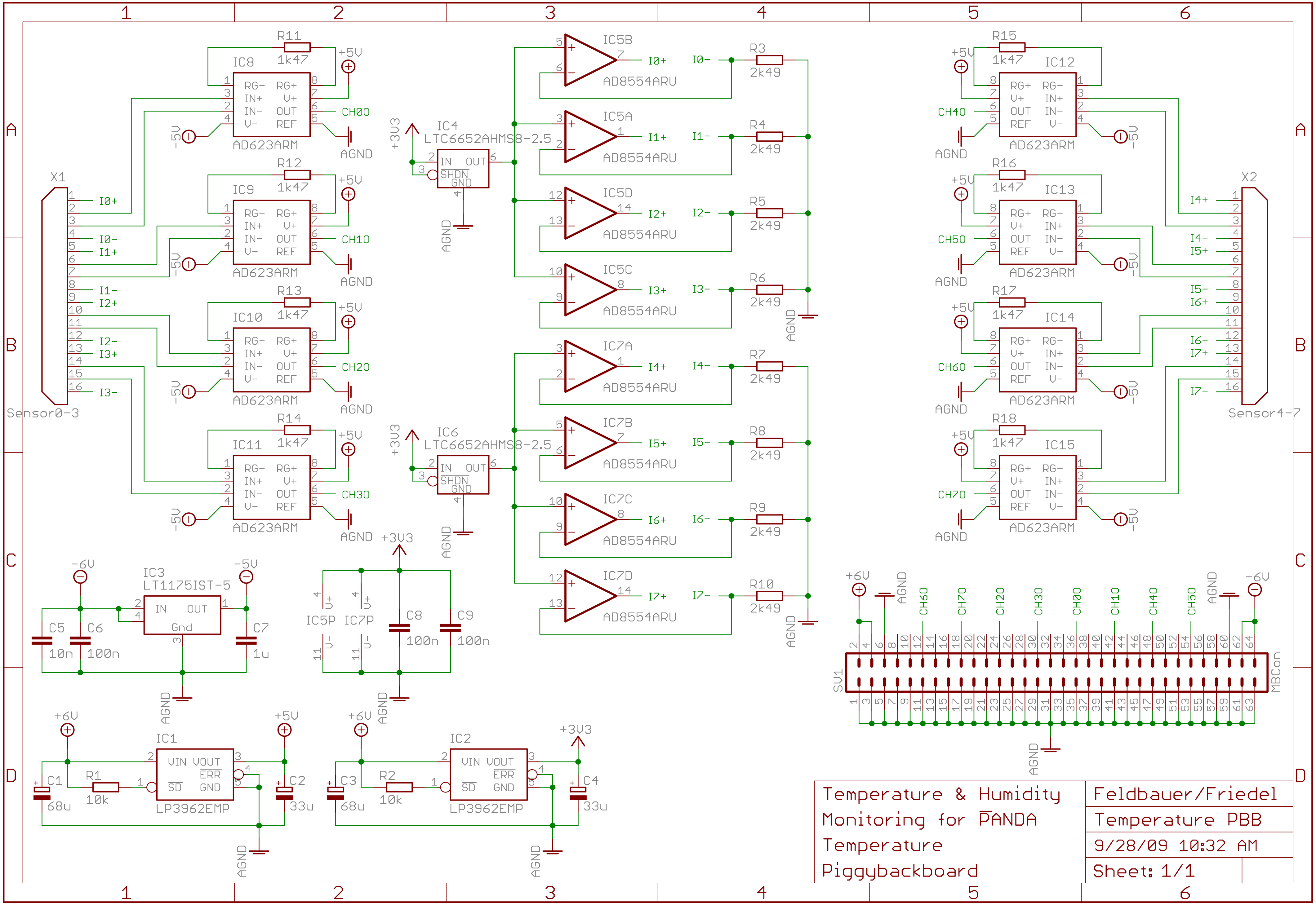
Temperature & Humidity
Monitoring for PANDA
Temperature
Piggybackboard
Feldbauer/Friedel
Temperature PBB
9/28/09 10:32 AM
Sheet: 1/1